ELSEVIER

Journal of Power Sources 75 (1998) 9–12

JOURNAL OF POWER SOURCES

# Tin-based oxide anode for lithium-ion batteries with low irreversible capacity

Kebao Wan [a], Sam F.Y. Li [a,b,*], Zhiqiang Gao [a], Kok Siong Siow [a]

[a] *Department of Chemistry, National University of Singapore, 10 Kent Ridge Crescent, Singapore 119260, Singapore*
[b] *Institute of Material Research and Engineering, National University of Singapore, 10 Kent Ridge Crescent, Singapore 119260, Singapore*

Received 24 February 1998; accepted 2 March 1998

**Abstract**

Several kinds of tin-oxide composites have been synthesised that can replace the carbon-based lithium intercalation materials as the anode of lithium-ion batteries. The electrochemical behaviour of these materials is investigated in ethylene carbonate and dimethyl carbonate (EC–DMC) based solutions containing lithium salts, $LiClO_4$. The lithium intercalation capacities in the tin-oxide materials prepared from the same raw materials and by the same method depend on the heat-treatment temperature. A higher charge capacity and lower irreversible capacity material based on $Sn_2P_2P_7$ is obtained by preparation at high temperature (700°C). The element manganese is added to these materials to obtain a material with lower irreversible capacity. This material ($SnMn_{0.5}PO_4$), prepared by the same method, exhibits a lower irreversible capacity. X-ray diffraction shows that this material has an amorphous structure. 

*Keywords:* Anode; Lithium-ion battery; Tin-oxide material; Irreversible capacity

## 1. Introduction

Lithium-ion batteries are suitable power sources for consumer electronics, primarily because of their high specific energy and energy density. They are now produced by several Japanese manufactures, and many other firms worldwide are engaged in their development. The anodes of these batteries use carbonaceous materials which were introduced to lithium-ion batteries by Nagaura and Tazawa [1]. The theoretical specific capacity of lithium intercalated graphite is 372 mA h $g^{-1}$. There have been important improvements in the specific capacity of carbonaceous materials that allow them to exceed the stoichiometric limit of lithium-ion intercalation in $LiC_6$. Some materials capable of creating high-capacity anodes which leapfrog this limit have been demonstrated via the deep doping of lithium [2–4]. Unfortunately, however, these materials deteriorate very quickly after a few charge–discharge operations [5,6].

Recently, Idota et al. [7] have synthesized an amorphous metal-oxide material which can store lithium ions with a columbic capacity that reaches the value given by hydrogen-storage alloys. This amorphous material is a metal composite oxide glass which contains tin(II). The advantages of this tin-oxide material are greater specific capacity and higher density compared with graphite. It provides a specific capacity of $> 600$ mA h $g^{-1}$ for reversible lithium adsorption and release, which corresponds to nearly twice the level of existing state-of-the-art carbonaceous materials. Courtney and Dahn [8] synthesized tin-oxide composite glasses, $Sn_2BPO_6$, which represent the smallest grains possible. The specific capacity of this material is close to 500 mA h $g^{-1}$. When these materials were used, batteries with higher specific capacity could be built. It was noticed, however, that the irreversible capacities of these tin-oxide materials in the first cycle were higher than that of carbonaceous materials. This will create difficulties if these tin-oxide materials are used as the anodes of commercial lithium-ion batteries.

In this work, tin-oxide composites, $Sn_2P_2O_7$, are synthesized at different heat-treatment temperatures. The electrochemical behaviour of these materials is measured. The element manganese is added and a material, $SnMn_{0.5}PO_4$, with a higher charge capacity and a lower irreversible capacity is obtained.

* Corresponding author.

0378-7753/98/$19.00 
*PII* S0378-7753(98)00076-7

## 2. Materials preparation

The $Sn_2P_2O_7$ materials were prepared by thermal decomposition of $SnHPO_4$ in argon at 500, 550, 600 and 700°C for 10 h. The crystal structures of the materials were analysed by means of X-ray diffraction (XRD).

To prepare the $SnMn_{0.5}PO_4$ material, stoichiometric amounts of $SnHPO_4$ and MnO were blended and heated in an alumina combustion boat within a furnace tube. The sample was heated in the furnace for 10 h and quenched to room temperature quickly. The material obtained was then subjected to grinding.

## 3. Electrochemical testing

Electrodes of the four materials were prepared by coating slurries of the respective powders (85 wt.%) graphite powder (10 wt.%, Aldrich) and polyvinylidene fluoride (5 wt.%, PVDF, Aldrich) dissolved in *N*-methyl pyrrolidinone (NMP, Aldrich) on to a nickel-foil substrate. The thickness of the coated film was ~70 μm. After the electrodes were dried for 4 h at 106°C and pressed between plates at $2.0 \times 10^6$ Pa, the electrodes were weighed. The area of the electrodes was 1.33 $cm^2$. The electrodes were incorporated in coin-type test batteries. The batteries used a polypropylene microsporous separator, an electrolyte [1 M $LiClO_4$ dissolved in a 50:50 vol.% (v/v) mixture of ethylene carbonate (EC, Fluka) and dimethyl carbonate (DMC, Fluka)] and a negative electrode of lithium foil (0.38-μm thick, 1.33 $cm^2$ area). Batteries were assembled and crimped-closed in an argon-filled glove box. All batteries were tested at a constant current of 0.1 mA $cm^{-2}$ and were charged and discharged between 0.01 and 1.2 V.

## 4. Results and discussion

### 4.1. XRD measurements

The diffraction patterns of the materials obtained at different temperatures are shown in Fig. 1. The peaks at 21.8, 27.2, 31.5 and 36.2°C show that the materials obtained at 500 to 700°C are due to the $Sn_2P_2O_7$ crystal. Microanalysis results confirm that these materials are $Sn_2P_2O_7$. Fig. 1 also shows that the peak intensity of $Sn_2P_2O_7$ decreases with increasing heat-treatment temperature, which shows that the grain size decreases with increasing heat-treatment temperature. The diffraction pattern for the material $SnMn_{0.5}PO_4$ is given in Fig. 2. There is no sharp peak in the pattern, which confirms its amorphous structure.

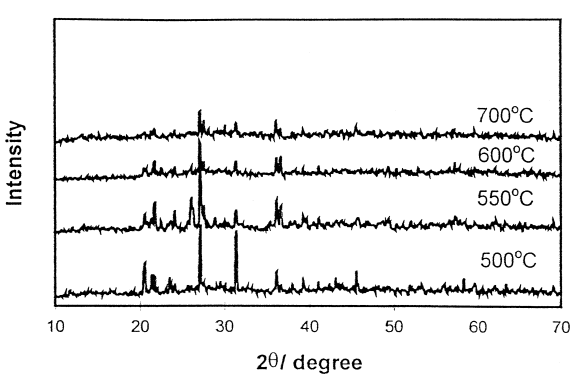


Fig. 1. Power XRD patterns of $Sn_2P_2O_7$ sample prepared at 500, 550, 600 and 700°C.

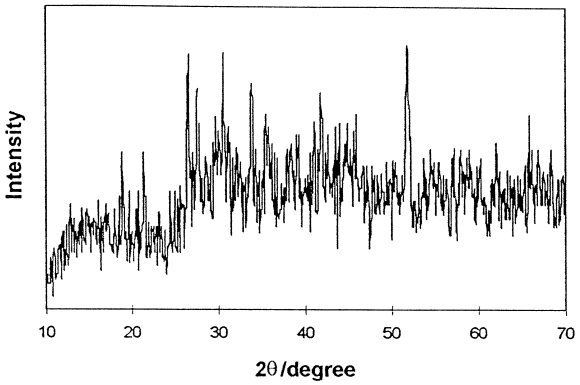


Fig. 2. Power XRD pattern of $SnMn_{0.5}PO_4$ sample prepared at 700°C.

### 4.2. IR spectra

The IR transmission spectra of $Sn_2P_2O_7$ and $SnMn_{0.5}PO_4$ in the range 400–1300 $cm^{-1}$ are given in Fig. 3. The transmission spectra of $Sn_2P_2O_7$ reveal a broad band centred at 1080 $cm^{-1}$ and several bands near 600 $cm^{-1}$. The band at 1080 $cm^{-1}$ is attributed to the symmetric stretching vibrations of the P–O–P chain and the bands at 540, 564 and 605 $cm^{-1}$ are attributed to the stretching Sn–O chain. Fig. 3 shows that the transmission spectrum of $SnMn_{0.5}PO_4$ has a band at 1020 $cm^{-1}$. The splitting of the P–O–P stretching, which is observed at 946, 1003, 1035, 1075 and 1090 $cm^{-1}$ of the $Sn_2P_2O_7$ transmission spectrum, is not present for $SnMn_{0.5}PO_4$. The band at 1020 $cm^{-1}$ is also attributed to the symmetric stretching vibrations of P–O–P chain. The centre of this band shifts from 1080 $cm^{-1}$ for $Sn_2P_2O_7$ to 1020 $cm^{-1}$

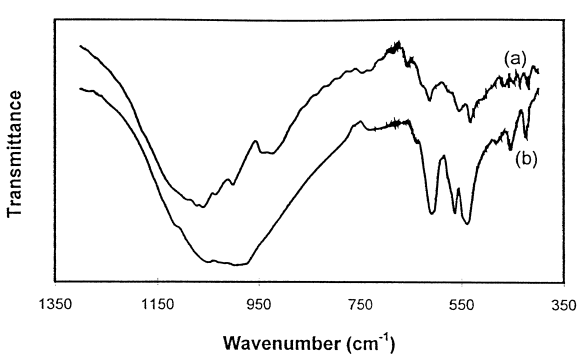


Fig. 3. IR transmission spectra of (a) $Sn_2P_2O_7$ and (b) $SnMn_{0.5}PO_4$ materials.

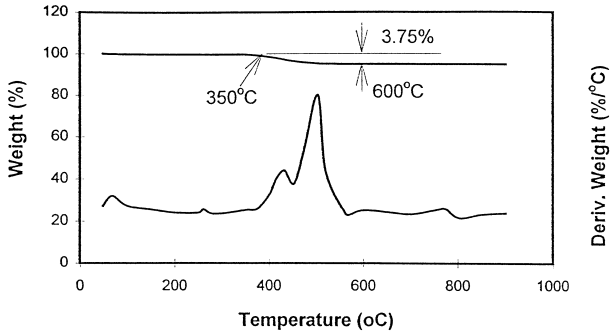


Fig. 4. TGA–DTA analyses of $SnMn_{0.5}PO_4$ material; 10°C $min^{-1}$ to 900°C in $N_2$.

for $SnMn_{0.5}PO_4$. The P–O–P band of the $SnMn_{0.5}PO_4$ is broader than its sharp counterpart in the spectra of $Sn_2P_2O_7$. The two bands at 372 and 445 $cm^{-1}$ are attributed to the stretching of the Mn–O chain; the bands are absent in the spectrum for $Sn_2P_2O_7$.

### 4.3. TGA–DTA measurements

TGA–DTA analysis was performed on the raw material for preparing $SnMn_{0.5}PO_4$ and the results are displayed in Fig. 4. The sample shows a mass loss between 350 and 600°C. This loss is due to the release of water by $SnHPO_4$. The reaction can be represented as follows:

$$SnHPO_4 + 1/2MnO \rightarrow SnMn_{0.5}PO_4 + 1/2H_2O \quad (1)$$

DTA shows two peaks at 432 and 511°C. The mass loss between 350 and 600°C is 3.75%, which is in agreement with 3.7 wt.% according to Eq. (1). After the mass loss at 600°C, TGA–DTA reveals no further mass loss for $SnMn_{0.5}PO_4$.

### 4.4. Electrochemical properties

Fig. 5 presents the first discharge–charge cycle for the battery $Li/Sn_2P_2O_7$ with different heat-treatment temperatures using a solvent of mixture of EC–DMC (1:1). $Sn_2P_2O_7$ was prepared at a heat-treatment temperature of 700°C. The shapes of the discharge–charge curves for the $Sn_2P_2O_7$ prepared at 500, 550 and 600°C are similar to that shown in Fig. 5. The dependence of the specific capacity of the first discharge–charge cycle on the heat-treatment temperature is given in Fig. 6. The discharge capacity increases when the heat-treatment temperature increases from 500 to 600°C. But when the heat-treatment temperature is increased further to 700°C, the discharge capacity decreases. The charge specific capacity of $Sn_2P_2O_7$ increases slightly with increasing heat-treatment temperature. The data show that the $Sn_2P_2O_7$ material synthesized at 700°C has a lower discharge capacity (1020 mA h $g^{-1}$) than that synthesized at 600°C (1140 mA h $g^{-1}$), but is higher than that of graphite material (theoretical specific capacity is 372 mA h $g^{-1}$). The charge capacity of the material synthesized at 700°C is higher (505 mA h $g^{-1}$) than that of material synthesized at 600°C (497 mA h $g^{-1}$) and of graphite materials. Thus, during the first cycle, the irreversible loss of capacity of this material is lower than that of material synthesized at 600°C, but is higher than that of graphite materials. The total loss of the irreversible capacity of $Sn_2P_2O_7$ material obtained at 700°C is 50%. The reason for these discharge–charge capacities changes may be attributed to structural effects because although all the samples are $Sn_2P_2O_7$ crystals, the grain size decreases with increasing heat-treatment temperature, as indicated by the XRD measurements in Fig. 1.

Although the specific capacity of the tin-oxide materials is higher than that of carbonaceous materials, the considerable irreversible capacity limits their use in lithium-ion batteries. To alleviate this problem, a new material was synthesized by adding the element manganese to the $Sn_2P_2O_7$ material. The charge–discharge cycle for a battery with $Li/SnMn_{0.5}PO_4$ and a solvent of mixture of EC–DMC (1:1) is shown in Fig. 7. The $SnMn_{0.5}PO_4$ was prepared at 700°C. The discharge–charge curve of this battery is similar to that of the battery with $Li/Sn_2P_2O_7$. After the battery was assembled, the open-circuit voltage was close to 3.0 V; this indicates that the tin-oxide electrode is in the de-lithiated state. Upon discharge, the battery voltage initially drops rapidly until it reaches about 1.55 V where it displays a plateau over a considerable range of specific capacity. The plateau at 1.55 V has been reported by Courtney and Dahn [8], who propose that it is related to reaction of lithium with oxygen bound to Sn to

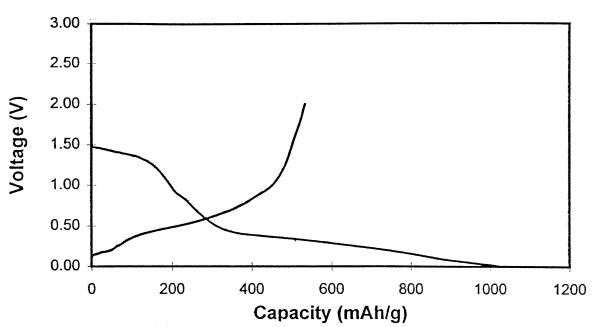


Fig. 5. Charge–discharge behaviour of $Sn_2P_2O_7$ prepared at 700°C in 1 M $LiClO_4$/EC-DMC (1:1) at 0.1 mA $cm^{-2}$.

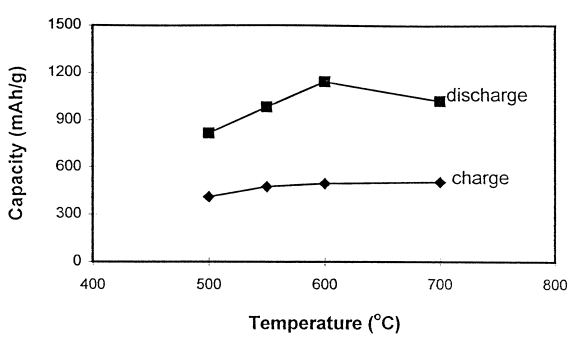


Fig. 6. Effect of heat-treatment temperature on charge–discharge capacity of tin-oxide material $Sn_2P_2O_7$.

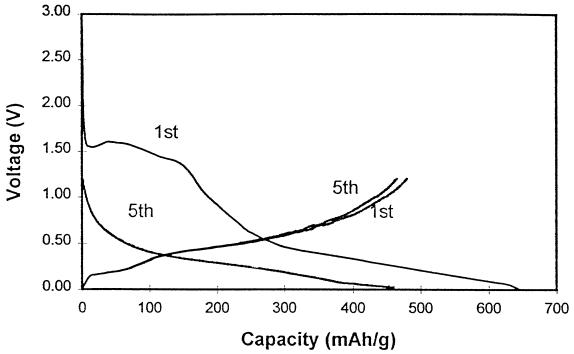


Fig. 7. Charge–discharge cyclic behaviour of $SnMn_{0.5}PO_4$ prepared at 700°C in 1 M $LiClO_4$/EC–DMC (1:1) at 0.1 mA $cm^{-2}$.

form $Li_2O$ and very small Sn regions. The majority of the discharge reaction occurs below 0.4 V after a sharp decline from 1.55 V. The shape of the charge curve exhibits a few differences from that for the battery with $Li/Sn_2P_2O_7$. During the first charge of the latter battery (Fig. 5), there is a plateau before the battery voltage reaches 0.3 V, which indicates the process of intercalation of lithium ions within the graphite powder. After that, the battery voltage increases rapidly until it reaches about 0.45 V. From this voltage, reversible lithium intercalation occurs as the voltage gradually increases to about 0.8 V. From then, the voltage starts to increase sharply towards the cut-off voltage of 1.2 V. The plateau at 1.6 V in the discharge curve is absent from the charge curve even if the cut-off voltage is 2.0 V. In Fig. 7, however, the battery voltage does not increase sharply after it reaches 0.8 V, but increases gradually from 0.45 V until it reaches near cut-off voltage of 1.2 V. Compared with $Sn_2P_2O_7$ synthesized at 700°C, the discharge-specific capacity of the tin-oxide material $SnMn_{0.5}PO_4$ of 635 mA h $g^{-1}$ is lower and the charge-specific capacity of 469 mA h $g^{-1}$ is almost equal to that of $Sn_2P_2O_7$. The irreversible capacity is 166 mA h $g^{-1}$. The total percentage of irreversible loss of capacity is 26%, which is lower than that of the material $Sn_2P_2O_7$, the tin-based oxide introduced by Idota et al. [7] and the material $Sn_2BPO_6$ introduced by Courtney and Dahn [8]. The percentage of irreversible capacity of these materials in the initial cycle is 40%.

The cyclic charge–discharge behaviour of $SnMn_{0.5}PO_4$ using a solvent of mixture of ethylene carbonate and dimethyl carbonate (EC–DMC) (1:1) is also shown in Fig. 7. After several cycles, no noticeable degradation of charge–discharge properties is observed. After the first cycle, there is no potential plateau at around 1.55 V, which is observed in the first cycle. These results show that the new tin-oxide material $SnMn_{0.5}PO_4$ is potentially a suitable material for use as the anode of lithium-ion batteries.

## 5. Conclusions

The results presented here show that the discharge–charge capacity of the tin-oxide material $Sn_2P_2O_7$ changes with the heat-treatment temperature and that the capacity is higher than that of graphite.

The material $SnMn_{0.5}PO_4$ has significant advantages over carbonaceous materials and other tin-oxide materials $Sn_2P_2O_7$ for use as the anode in lithium-ion batteries. Not only does it have a high reversible specific capacity but, most importantly, it also shows lower irreversible capacity than other tin-oxide materials.

## References

[1] T. Nagaura, K. Tazawa, Prog. Batteries Sol. Cells 9 (1990) 20.
[2] A. Mabuchi, K. Tokumitsu, H. Fujimoto, T. Kasuh, J. Electrochem. Soc. 142 (1995) 1041.
[3] K. Sato, M. Noguchi, A. Demachi, N. Oki, M. Endo, Science 264 (1994) 556.
[4] S. Yata, H. Kinoshita, M. Komori, N. Ando, T. Kashiwamura, T. Harada, K. Tanaka, T. Yamabe, Synth. Met. 62 (1994) 153.
[5] Z.X. Shu, R.S. Mcmillan, J.J. Murray, J. Electrochem. Soc. 140 (1993) 922.
[6] W. Li, J.R. Dahn, D.S. Wainwright, Science 264 (1994) 1115.
[7] Y. Idota, T. Kubota, A. Matsufuji, Y. Maekawa, T. Miyasaki, Science 276 (1997) 1395.
[8] I.A. Courtney, J.R. Dahn, J. Electrochem. Soc. 144 (1997) 2943.